J. Quant. Spectrosc. Radiat. Transfer. Vol. 5, pp. 369–390. Pergamon Press Ltd., 1965. Printed in Great Britain

POTENTIAL ENERGY CURVES FOR N_2, NO, O_2 AND CORRESPONDING IONS

FORREST R. GILMORE

The RAND Corporation, Santa Monica, California
(*Received* 8 *October* 1964)

I. INTRODUCTION

CURVES of the potential energy versus internuclear distance form a convenient way of displaying the energy levels of diatomic molecules. In addition, they permit the ready application of the Franck–Condon principle to radiative transitions, electron–molecule collisions, predissociations, etc. Such curves for atmospheric molecules and molecular ions are helpful in determining the thermodynamic properties and radiation and reaction rates of heated or excited air.

Conventionally, potential-energy curves are fit by the simple Morse functions,[1,2] although it has long been realized that this function often gives a poor fit at internuclear distances somewhat greater than the equilibrium distance. Recently, VANDERSLICE, MASON and MAISCH[3] have modified a method due to RYDBERG,[4] KLEIN,[5] and REES[6] to permit numerical calculation of accurate potential curves over the range for which spectroscopic data are available. VANDERSLICE, *et al.* applied their method to many of the lower states of N_2, NO and O_2.[7–9] In the present work, a simpler numerical modification of the Rydberg–Klein method (not requiring the quadratic-fitting of Rees) was derived and applied to these same states and others, including the known states of the molecular ions.

As a check, a series recently derived by JARMAIN[10] for computing potential curves from the conventional "spectroscopic constants" was also applied to these states. Although JARMAIN made numerical calculations[11] only for the lowest parts of potential curves, suspecting that his series was inaccurate for higher portions, results using his series were found to agree very well with Rydberg–Klein results up to about two-thirds of the dissociation energy for each state, as long as the spectroscopic constants used fit the observed energy levels this high. However, in many cases the published spectroscopic constants had to be modified to obtain such a fit.

For predicted but unobserved electronic states, or observed states above the highest observed energy level, recourse must be made to theoretical considerations or to indirect experimental evidence. In the present work an attempt has been made to use all available information in drawing the curves for these states: published data on perturbations, predissociations, and excitation energies; published quantum-mechanical calculations; simple molecular-orbital principles relating unknown states to similar known states;[2,12] and rules determining the (atomic) dissociation limits of the various molecular states.[2,13]

In the present report the basic data and methods are discussed only briefly, and the results are presented graphically. Future reports will discuss the data and methods more fully, and will present the results numerically, including revised spectroscopic constants for some of the states. It is also hoped that, as results of spectroscopic investigations currently underway at other laboratories become available, a considerable extension of the present work will be possible.

II. CALCULATION OF POTENTIAL-ENERGY CURVES FROM SPECTROSCOPIC DATA

RYDBERG[4] and KLEIN[5] express the two internuclear distances, r_1 and r_2, corresponding to a given potential energy* of a diatomic molecule as

$$r_1, r_2 = (f^2+f/g)^{1/2} \pm f, \tag{1}$$

where f and g are the partial derivatives of an integral S, which is a function of the energy and angular momentum of the molecule. However, it is more convenient to introduce explicitly the rotational and vibrational quantum numbers J and v, and to express the potential energy U in spectroscopic units of cm^{-1}. With these modifications, and using standard spectroscopic notation,[2] Rydberg's integral becomes

$$S(U, J) = \frac{h\sqrt{(hc)}}{\pi\sqrt{(2\mu)}} \int_{-1/2}^{v} [U - T(v', J)]^{1/2} \, dv', \tag{2}$$

where $T(v', J)$ is the term value (energy of a given v', J level) and the upper limit v satisfies $T(v, J) = U$. Since the Rydberg–Klein method is a semiclassical procedure, the quantum numbers J and v must be treated as continuous.

The partial derivatives f and g may now be expressed explicitly in terms of the conventional spectroscopic constants. For the rotationless ($J = 0$) state one obtains f and g in terms of the vibrational levels $G(v)$ and rotational constants B_v:

$$f(v) = \frac{1}{hc}\left[\frac{\partial S}{\partial U}\right]_{J=0} = \frac{1}{2\pi\sqrt{(2\mu c/h)}} \int_{-1/2}^{v} [G(v) - G(v')]^{-1/2} \, dv', \tag{3}$$

$$g(v) = -\frac{8\pi^2\mu}{h^2}\left[\frac{\partial S}{\partial J(J+1)}\right]_{J=0} = 2\pi\sqrt{(2\mu c/h)} \int_{-1/2}^{v} B_{v'}[G(v) - G(v')]^{-1/2} \, dv', \tag{4}$$

since $U = T(v, 0) = G(v)$ + constant, and $[\partial T/\partial J(J+1)]_{J=0} = B_v$. Using the experimental values of $G(v)$ and B_v, the quantities f and g can be evaluated directly by numerical quadrature, except for two minor difficulties.

The first difficulty is that the integrands have integrable singularities at the upper limit. Several methods could be used to overcome this difficulty; the method used here

* Actually, this is an "effective" potential energy for rotation and vibration of the molecule; it includes both the electrostatic potential energy of the electrons and nuclei and the kinetic energy of the electrons.

was to write the integrand in equation (3) as $(v-v')^{1/2}(G_v-G_{v'})^{1/2}/(v-v')^{1/2}$ and to fit the numerator of this expression between $v' = v-3/2$ and $v' = v$ by a quadratic in $v-v'$ which fits exactly at $v-1$, $v-\frac{1}{2}$ and v. This part of the integral can then be evaluated in terms of the G's, without specific reference to the coefficients of the quadratic fit:

$$\int_{v-3/2}^{v} (G_v-G_{v'})^{-1/2}\,\mathrm{d}v' = \sqrt{(6/5)}[(G_v-G_{v-1})^{-1/2} + 2^{-3/2}(G_v-G_{v-1/2})^{-1/2}+(3G_v-4G_{v-1/2}+G_{v-1})^{-1/2}], \quad (5)$$

where $G(v)$ is written G_v for convenience. The expression for the integral in equation (4) is similar except that the three terms on the right hand side have additional factors of B_{v-1}, $B_{v-1/2}$, and B_v, respectively.

The second difficulty is that the $G(v)$ and B_v values must be extrapolated to $v = -\frac{1}{2}$ (which corresponds to the minimum or equilibrium point on the potential curve), and usually interpolated for nonintegral values of v to get accurate values for f and g. However, this does not present a significant complication. Experience has shown the great desirability of plotting the available experimental $G(v)$ and B_v values and drawing the best smooth curves through the data. In most cases, the deviations of the points from the smooth curves are due to experimental inaccuracy, as often indicated by the differences between results of different investigators, or between the results of the same investigator's measurements on different bands.

Occasionally, real deviations from a smooth curve are found. These are due to the "perturbations" which occur when a vibrational level of one electronic state happens to fall close to that of another state of the same symmetry and multiplicity. Perturbations which affect a group of consecutive vibrational levels smoothly will not prevent the drawing of smooth $G(v)$ and B_v curves, nor the calculating of corresponding potential-energy curves, even though the curves may have unusual shapes. Perturbations involving isolated vibrational levels cannot be accurately handled by the Rydberg–Klein method; however, such perturbed electronic states cannot really be represented precisely by potential-energy curves. If the requirement of smoothness is relaxed, many different potential curves would give the same (rotationless) vibrational levels, but no curve would give all the rotational levels properly, because the degree of perturbation depends upon the v and J values individually and not just on the potential energy. In such cases, it is probably best to calculate "unperturbed" potential energy curves by ignoring the perturbed energy levels, so that smoothed $G(v)$ and B_v curves should again be used.

After smoothed $G(v)$ and B_v curves are drawn, it is easy to read them at integral and half-integral values of v, or even closer if desired (or to use some interpolation scheme), and then apply Simpson's rule together with equation (5) to evaluate the integrals in equations (3) and (4). This method is less laborious than the quadratic-fitting method of VANDERSLICE, MASON and MAISCH.[3]

In the present work, experimental values of B_v and the vibrational-level differences, ΔG, for the various electronic states of N_2, N_2^+, O_2 were plotted on a large scale. Smooth "best value" curves were drawn, taking into account the self-consistency and quoted accuracy of each investigator's work. When fewer B_v than ΔG values were available, the B_v curves were extrapolated smoothly over the experimental ΔG range. Values of $G(v)$

and B_v were then read from the curves at $v = -\frac{1}{2}, 0, 1, 2, \ldots$ and fed into a Fortran program which first calculated $G(v)$ at half-integral v values by quadratic interpolation and B_v by linear interpolation. Next, the values r_1 and r_2 were calculated for vibrational levels from $v = 1$ to the highest observed level, using equations (1) to (5). The same program also calculated r_1 and r_2 for as many integral or non-integral values of v as desired using input spectroscopic constants (ω_e, $\omega_e x_e$, $\omega_e y_e$, $\omega_e z_e$, B_e, α_e, γ_e) and JARMAIN's series[10] for f and g. The r_1 and r_2 values calculated by the two methods agreed within 0·0001 Å up to about half the dissociation energy of each state, and within 0·0003 Å up to about two-thirds of the dissociation energy, as long as the spectroscopic constants used fit the input $G(v)$ and B_v values this far.

The potential energies calculated in the present work here were also compared where possible with the Rydberg–Klein–Rees calculations of VANDERSLICE *et al.*,[7–9] and with the calculations by JARMAIN[11] using his series, although neither of these investigators included as many electronic states as are treated here. The present values of r_1 and r_2 generally agreed within 0·003 Å with those of the previous investigators, except where the latter used older or less-accurate spectroscopic data.

Frequently, many higher vibrational levels of a state have been observed for which no rotational analysis has been carried out. In such cases, the Rydberg–Klein and Jarmain results may give potential curves which unrealistically double back or have an inflection point at small internuclear distances, due to inaccuracies in extrapolating B_v values. Fortunately, the curve is usually so steep in this region that a direct extrapolation of the r_1 values can be made with good accuracy. Since, by equations (1) and (3), the difference $r_2 - r_1$ depends only on the vibrational intervals, the r_2 values can then be determined with the help of the Rydberg–Klein or Jarmain results.

III. ESTIMATION OF UNOBSERVED OR INCOMPLETELY OBSERVED STATES

The general theoretical principles used for estimating the energy levels of diatomic molecules from their electron configurations have been discussed in detail in MULLIKEN's classical review,[12] while a shorter account may be found in the book by HERZBERG.[2] The accuracy of these estimates depends considerably upon the availability of experimental values for related electronic states of the same or similar molecules. Because of the great experimental progress made in the last few years, considerably better estimates for the remaining unobserved states can now be made. Revised estimates for nitrogen were made a few years ago by MULLIKEN,[13] but already some of his values have been superseded by later data.

Another source of energy-level information is the quantum-mechanical treatment of molecules from basic principles. However, even the most elaborate calculations carried out so far, such as two recent self-consistent-field calculations for various electronic states of nitrogen,[14,15] give values which are often in error by more than 1 eV, although the relative positions of similar states may be determined with greater accuracy. Moreover, the published calculations apply primarily to the well-known states, omitting most of the predicted but unobserved states.

The above remarks apply to small and moderate internuclear distances. At somewhat larger internuclear distances, both rough estimation and more-accurate calculation

usually become more difficult because simple molecular-orbital configurations become poor approximations to the actual states. Recently a few workers have treated several states of present interest at large internuclear distances using the valence-bond approximation. Although, as indicated specifically in Section V, some of these results have been used here for lack of anything better, they should be viewed with caution. Not only do they involve numerical approximations (mentioned in the original papers), they also neglect interactions between electronic configurations and ignore the possibility that the separated "valence-bond atoms" do not coincide with ground-state atoms. MULLIKEN[16] has recently shown that, at least in one particular case, neither of these omissions is justified.

Indirect experimental evidence on some molecular states can be obtained from perturbations, predissociations and electron-impact data. The principles of the first two phenomena are discussed by HERZBERG,[2] while the last is treated by CRAGGS and MASSEY.[17] Where such data were used in the present work, details are given below in Section V.

IV. DETERMINATION OF DISSOCIATION LIMITS

As the internuclear distance is increased, the potential energy of a diatomic molecule or molecular ion approaches the energy of the separated atoms or atomic ions. The ground electronic states of most molecules dissociate into atoms in their ground state. The energy difference, measured from the $v = 0$ level of the molecule, is known as the dissociation energy of the molecule. By a variety of methods[18] the dissociation energy of nitrogen has been determined to be $78{,}717 \pm 40$ cm^{-1} (or $9{\cdot}759 \pm 0{\cdot}005$ eV, using the latest conversion factor[19]) and that of oxygen[20] to be $41{,}260 \pm 15$ cm^{-1} ($5{\cdot}115 \pm 0{\cdot}002$eV). These values may be combined with the thermochemical value of $21{\cdot}46 \pm 0{\cdot}04$ kcal/mole (7506 ± 14 cm^{-1}) for the heat of formation of nitric oxide[21] at 0°K to obtain a value of $52{,}483 \pm 40$ cm^{-1} ($6{\cdot}507 \pm 0{\cdot}005$ eV) for the dissociation energy of nitric oxide.

Having thus obtained values for the lowest dissociation limits of the molecules, one may readily calculate the energies of the higher limits (corresponding to dissociation into excited atoms or ions) by adding the energies of atomic excitation or ionization given by MOORE.[22] In the present work the multiplet (spin-orbit) splitting of the atomic and molecular states has been neglected, and a weighted average over the individual levels used. The total splitting does not exceed 0·02 eV in the cases considered. The only needed atomic energy levels not given by Moore are those of the negative ions N^- and O^-. These were determined from the electron affinities of $-0{\cdot}27 \pm 0{\cdot}11$ eV calculated by CLEMENTI and MCLEAN[23] for N, and $1{\cdot}465 \pm 0{\cdot}005$ eV measured by BRANSCOMB *et al.*[24] for 0.

The remaining problem is to determine which dissociation limit applies to each electronic state of the molecule. The number and types of molecular states which can be formed from each pair of atomic states can be determined from well-established theoretical principles.[2,12] If the "noncrossing rule"[2,25] is rigorous the correlation of molecular states with dissociation limits is simple: each state goes to the lowest available limit not pre-empted by a lower state of the same type. However, it is known that some states (such as NO $A\,^2\Sigma^+$) have potential curves which tend to approach a higher dissociation limit before (presumably) turning down to a lower limit. Such behavior is well established for Rydberg states (states having one electron in an outer orbital): the lower portions of their

potential curves have the same shape as that of the corresponding molecular-ion core. A few other cases of curves with potential maxima or other peculiarities are also known. These peculiarities are generally understandable theoretically as the result of a change in electronic configuration as the internuclear distance goes from small to large values, but no simple theory is available to predict the curve shape at moderately large internuclear distances in any detail.

In the present work a few curves have been drawn with potential maxima, based on experimental evidence or published valence-bond calculations, but curves for all other states have simply been extrapolated smoothly and monotonically to the lowest permissible dissociation limit.

V. RESULTS AND DISCUSSION

The calculated and estimated potential energy curves for nitrogen, nitric oxide and oxygen are presented in Figs. 1, 2, and 3, respectively. Less-accurate portions of the curves are shown dashed or dotted. Observed vibrational levels are indicated by short horizontal lines extending inward from the potential curves. In all cases the zero of energy is taken to be that of the $v = 0$ level of the ground-state neutral molecule. Observed transitions among the electronic states shown in the figures are listed Table 1, while Tables 2, 3, and 4 give the probable molecular-orbital electron configurations of the states (except states shown only by short broken curves near the dissociation limits). The data and methods used to obtain the potential curves will be discussed briefly below.

The unstable N_2^- *ion*

According to molecular-orbital theory, the ground state of the N_2 molecule has closed outer electronic shells, so that its electron affinity should be negative and the ground state of N_2^- should be unstable against disintegration into N_2+e. In agreement with this theory, the N_2^- ion has never been identified in mass-spectrographic investigations. However, the electron-scattering experiments of SCHULZ[26] in nitrogen can be interpreted as indicating the temporary formation of an N_2^- state having a lifetime at least as long as a vibrational period (i.e. $\gtrsim 10^{-14}$ sec). Hence, the potential curve for such a state may have some physical significance.

The predicted ground state of N_2^- is $^2\Pi_g$, with a potential curve similar to the ground states of the isoelectronic NO and O_2^+ molecules, and a dissociation limit about 0·3 eV above the lowest dissociation limit of N_2, due to the negative electron affinity of the nitrogen atom.[23] The minimum of the N_2^- curve should thus lie 2 or 3 eV above that of N_2, which agrees reasonably well with SCHULZ's value of 1·6 eV for the inelastic threshold.[26] The N_2^- curve in Fig. 1 is drawn with a shape similar to those of NO and O_2^+, a depth based on Schulz's data, and a minimum at 1·18 Å, consistent with the isoelectronic series $r_e(O_2^+) = 1{\cdot}12$ Å, $r_e(NO) = 1{\cdot}15$ Å. This value for r_e also yields Franck–Condon factors which peak at $v = 2$ (2·1 eV), consistent with the peak found by Schulz.*

* The probability of electron energy loss by the process $N_2(v''=0)+e \rightarrow N_2^-(v') \rightarrow N_2(v''>0)+e$ is proportional to $q(1-q)$, where $q = q(v', 0)$ is the relevant Franck–Condon factor (square of the vibrational overlap integral), and the sum rule has been used to write the probability of the second step as $(1-q)$. As v' is varied, the total probability has a maximum where q has a maximum, as long as $q \leqslant 0{\cdot}5$, which holds here. Approximate Franck–Condon factors may be readily obtained by the use of BATES' tables.[27]

No potential curves are shown for excited states of N_2^- since such states are probably so short-lived that their curves would have no real significance.

TABLE 1. OBSERVED TRANSITIONS AMONG THE ELECTRONIC STATES SHOWN IN FIGS. 1, 2, AND 3.*

Permitted Transitions	Forbidden Transitions
Nitrogen	
N_2 $B \rightleftarrows A$ (First positive bands)	N_2 $A \rightleftarrows X$ (Vegard–Kaplan bands)
N_2 $C \rightarrow B$ (Second positive bands)	N_2 $a \rightleftarrows X$ (Lyman–Birge–Hopfield bands)
N_2 $C' \rightarrow B$ (Goldstein–Kaplan bands)	N_2 $B' \rightleftarrows X$ (Wilkinson–Ogawa–Tanaka I bands)
N_2 $E \rightarrow A$ (γ bands)	N_2 $a' \rightleftarrows X$ (Wilkinson–Ogawa–Tanaka II bands)
N_2 $B' \rightarrow B$ (Y bands)	N_2 $C \leftarrow X$ (Tanaka bands)
N_2 $b' \rightleftarrows X$ (Birge–Hopfield bands†)	
N_2 $A \rightarrow X$ (Meinel bands)	
N_2^+ $B \rightarrow X$ (First negative bands)	
N_2^+ $C \rightarrow X$ (Second negative bands)	
N_2^+ $D \rightarrow A$ (Janin–d'Incan bands)	
Nitric Oxide	
NO $A \rightleftarrows X$ (γ bands)	NO $a \rightarrow X$ (M bands)
NO $B \rightleftarrows X$ (β bands)	
NO $C \rightleftarrows X$ (δ bands)	
NO $D \rightleftarrows X$ (ϵ bands)	
NO $B' \rightleftarrows X$ (β' bands)	
NO $E \rightleftarrows X$ (γ' bands)	
NO $F, G, K, M, S \leftarrow X$ (Lagerquist–Miescher bands)	
NO $H, H' \leftarrow X$ (Huber–Miescher bands)	
NO $b \rightarrow a$ (Ogawa bands)	
NO $C \rightarrow A$ (Heath band)	
NO $D \rightarrow A$ (Feast bands)	
NO $E \rightarrow A$ (Duffieux–Grillet–Feast bands)	
NO $H, H' \rightarrow A$ (Tanaka–Miescher bands)	
NO $B' \rightarrow B$ (Tanaka–Ogawa bands)	
NO $H, H', F \rightarrow C$ (Feast–Lagerquist–Miescher bands)	
NO $E, H, H' \rightarrow D$ (Feast–Heath bands)	
NO^+ $A \rightarrow X$ (Miescher–Baer bands)	
Oxygen	
O_2 $B \rightleftarrows X$ (Schumann–Runge bands)	O_2 $a \leftarrow X$ (Infrared atmospheric bands)
O_2^+ $A \rightarrow X$ (Second negative bands)	O_2 $b \rightleftarrows X$ (Atmospheric bands)
O_2^+ $b \rightarrow a$ (First negative bands)	O_2 $A \rightleftarrows X$ (Herzberg bands)
O_2^+ $c \rightarrow b$ (Hopfield's emission bands)	O_2 $c \leftarrow X$ (Herzberg II bands)
	O_2 $C \leftarrow X$ (Herzberg III bands)
	O_2 $b \rightarrow a$ (Noxon band)
	O_2 $A \rightarrow b$ (Broida–Gaydon bands)

* For several N_2 and NO band systems having no commonly-accepted names, names are suggested here, based on priority of discovery and analysis, and avoidance of duplication.

† Both $b \rightleftarrows X$ and $b' \rightleftarrows X$ bands are usually denoted Birge–Hopfield bands[28,40] after their discoverers, although in Fig. 196 of Herzberg[2] the $b' \rightleftarrows X$ bands are called Worley bands.

The N_2 molecule

Potential curves for the well-known lower states of N_2, in the region of their observed vibrational levels, have been calculated using the numerical Rydberg–Klein method described in Section II. The required $G(v)$ and B_v values were taken from the literature, which has recently been summarized by WALLACE.[28] In addition to the references cited by Wallace, some recent work of TANAKA, OGAWA and JURSA[29] was used. The present Rydberg–Klein results agree within 0·003 Å with the less-complete results of VANDERSLICE, MASON and LIPPINCOTT[7] except for differences of up to 0·022 Å in the $A\,^3\Sigma_u^+$ state and up to 0·005 Å in the $C\,^3\Pi_u$ state due to use of newer spectroscopic data.

TABLE 2. MOLECULAR-ORBITAL ELECTRON CONFIGURATIONS OF NITROGEN

Molec.	Electron configuration* state	$1\pi_u$	$3\sigma_g$	$1\pi_g$	$3\sigma_u$	other	Molec.	Electron configuration* state	$1\pi_u$	$3\sigma_g$	$1\pi_g$	$3\sigma_u$	other
N_2^-	$X\,^2\Pi_g$	4	2	1	0		N_2^+	$X\,^2\Sigma_g^+$	4	1	0	0	
N_2	$X\,^1\Sigma_g^+$	4	2	0	0			$A\,^2\Pi_u$	3	2	0	0	
	$A\,^3\Sigma_u^+$	3	2	1	0			$B\,^2\Sigma_u^+$	4	2	0	0	$-2\sigma_u$
									3	1	1	0	
	$^3\Delta_u$	3	2	1	0			$^4\Sigma_u^+$	3	1	1	0	
	$B\,^3\Pi_g$	4	1	1	0			$^4\Delta_u$	3	1	1	0	
	$B'\,^3\Sigma_u^-$	3	2	1	0			$D\,^2\Pi_g$	2	2	1	0	
									4	0	1	0	
	$a'\,^1\Sigma_u^-$	3	2	1	0			$^4\Sigma_u^-$	3	1	1	0	
	$a\,^1\Pi_g$	4	1	1	0			$^4\Pi_g$	2	2	1	0	
	$w^1\Delta_u$	3	2	1	0			$C\,^2\Sigma_u^+$	3	1	1	0	
									4	2	0	0	$-2\sigma_u$
	$^5\Sigma_g^+$	2	2	2	0			$^2\Delta_u$	3	1	1	0	
		3	1	1	1			$^4\Pi_u$	1	2	2	0	
	$^7\Sigma_u^+$	2	1	2	1				3	0	2	0	
								$^4\Sigma_g^+$	2	1	2	0	
	$C\,^3\Pi_u$	4	2	1	0	$-2\sigma_u$		$^2\Sigma$	3	1	1	0	
	$^5\Pi_u$	3	1	2	0			$^2\Pi_u$	1	2	2	0	
	$E\,^3\Sigma_g^+$	4	1	0	0	$3s\sigma_g$			3	0	2	0	
	$C'\,^3\Pi_u$	3	1	2	0								
	$b'\,^1\Sigma_u^+$	3	2	1	0								

* The valence-shell orbitals are listed here in the usual order of their binding energies, for internuclear distances less than about 1·4 Å. For larger distances, however, the $3\sigma_g$ orbital is usually more tightly bound than the $1\Pi_u$ orbital. All states include $(1\sigma_g)^2(1\sigma_u)^2(2\sigma_g)^2(2\sigma_u)^2$ electrons, except that states marked $-2\sigma_u$ have only one $2\sigma_u$ electron. The configurations listed are those believed to be the dominant contributors near the potential minimum of each state.

In Fig. 1 the long-range "tail" of the $X\,^1\Sigma_g^+$ curve and all of the repulsive $^7\Sigma_u^+$ curve are taken from the valence-bond calculations of MEADOR,[30] which appear to be more accurate than those of VANDERSLICE, MASON and LIPPINCOTT.[7] The loosely-bound $^5\Sigma_g^+$ curve is taken from CARROLL,[31] who put together the indirect experimental evidence.

The predicted but still unobserved $^3\Delta_u$ state is placed by molecular-orbital calculations[14,15] halfway between the $A\,^3\Sigma_u^+$ and the $B'\,^3\Sigma_u^-$ states. KENTY[32] has presented arguments for an excited state of N_2 between 7·9 and 8·3 eV and a lifetime of 1–2 sec, and suggested that this is the $^3\Delta_u$ state. However, this energy is significantly higher than that predicted for the $^3\Delta_u$ state, and any $^3\Delta_u$ levels this high should have a lifetime much

shorter than 1 sec due to radiative transitions to the $B\,^3\Pi_g$ state. Moreover, KING and GATZ[33] have presented alternative explanations of Kenty's experimental data.

The dashed curve labelled $^5\Pi_u$ on Fig. 1 corresponds to CARROLL's[34] curve for the state which predissociates the $C\,^3\Pi_u$ state, and which BÜTTENBENDER and HERZBERG[35] suggested was also a $^3\Pi_u$ state. However, if this suggestion were correct it would be very surprising that bands connecting this state with $B\,^3\Pi_g$ have not been observed and that strong perturbations of the $C\,^3\Pi_u$ levels do not occur. A $^5\Pi_u$ state is predicted theoretically[13,14] in this energy region, and provides a more plausible explanation for the observed predissociation.

TABLE 3. MOLECULAR-ORBITAL ELECTRON CONFIGURATIONS FOR NITRIC OXIDE

Molec.	Electron configuration* state	3σ	1π	$1\pi^*$	$3\sigma^*$	other	Molec.	Electron configuration* state	3σ	1π	$1\pi^*$	$3\sigma^*$	other
NO^-	$X\,^3\Sigma^-$	2	4	2	0		NO	$K\,^2\Pi$	2	4	0	0	$4p\pi$
	$^3\Pi$	2	4	1	1			$M\,^2\Sigma^+$	2	4	0	0	$5p\sigma$
		1	4	3	0								
NO	$X\,^2\Pi_r$	2	4	1	0			$^4\Pi_i$	2	2	3	0	
	$a\,^4\Pi_i$	2	3	2	0			$^2\Sigma^+$	2	4	0	1	
									1	4	2	0	
	$A\,^2\Sigma^+$	2	4	0	0	$3s\sigma$		$S\,^2\Sigma^+$	2	4	0	0	$5s\sigma$
	$B\,^2\Pi_r$	2	3	2	0		NO^+	$X\,^1\Sigma^+$	2	4	0	0	
	$b\,^4\Sigma^-$	1	4	2	0			$a\,^3\Sigma^+$	2	3	1	0	
	$C\,^2\Pi$	2	4	0	0	$3p\pi$		$^3\Delta$	2	3	1	0	
	$D\,^2\Sigma^+$	2	4	0	0	$4p\sigma$		$^3\Pi$	1	4	1	0	
	$^2\Sigma^+$	1	4	2	0			$A\,^1\Pi$	1	4	1	0	
		2	4	0	1								
	$^4\Sigma^+$	2	3	1	1			$^3\Sigma^-$	2	3	1	0	
		1	3	3	0								
	$^2\Phi_i$	2	3	2	0			$^1\Sigma^-$	2	3	1	0	
	$B'\,^2\Delta_i$	1	4	2	0			$^1\Delta$	2	3	1	0	
	$E\,^2\Sigma^+$	2	4	0	0	$4s\sigma$		$^5\Sigma^+$	2	2	2	0	
	$F\,^2\Delta$	2	4	0	0	$3d\delta$			3	1	1	1	
	$G\,^2\Sigma^-$	1	4	2	0			$^7\Sigma^+$	1	2	2	1	
	$H\,^2\Sigma^+$	2	4	0	0	$4d\sigma$		$^1\Sigma^+$	2	3	1	0	
	$H'\,^2\Pi$	2	4	0	0	$4d\pi$		$^3\Sigma^+$	2	2	2	0	

* The valence-shell orbitals are listed here in the usual order of their binding energies for nitric oxide. All states include $(1\sigma)^2(1\sigma^*)^2(2\sigma)^2(2\sigma^*)^2$ electrons. For Rydberg orbitals a semi-united-atom notation is used (R. S. MULLIKEN, to be published), which is more appropriate than the separated-atom notation used by HUBER and MIESCHER.[64]

According to Fig. 1 the (0, 0) band of the $^5\Pi_u \rightarrow {}^5\Sigma_g^+$ transition should lie at about 7000 Å. LOFTHUS[36] has observed an emission band at 6895·5 Å between unidentified states having rotational constants about like those expected for these quintet states. However, since the observed band had only single branches, such an identification would require the multiplet splitting of the $^5\Pi_u$ state to be very small, which appears to disagree with theoretical expectations and with details of the observed $C\,^3\Pi_u$ predissociation. This question needs further study.

HEPNER and HERMAN[37] have observed new nitrogen bands in the infrared lead-sulfide region, and suggested a $^5\Pi \rightarrow {}^5\Sigma$ interpretation. However, their data indicate two

states less than 1 eV apart and each having a dissociation energy greater than 1 eV, so they can hardly be the quintet states considered here. For a different possible interpretation of the Hepner–Herman bands, see the N_2^+ quartet discussion, below.

The Rydberg–Klein calculations for the $C\,^3\Pi_u$ state give a curve which starts to bend over above the $v = 2$ level. For this reason, and to satisfy the noncrossing rule, the curves of this state and the $C'\,^3\Pi_u$ state recently analyzed by CARROLL[34] have been joined into a single $^3\Pi_u$ curve with a double minimum, similar to some H_2 curves recently discovered by DAVIDSON.[38] The so-called $v = 5$ level of the C state and $v = 1$ level of the C' state[28] are not shown on Fig. 1 because they may belong either to the combined $C-C'$ states (lying above the hump that separates the two states) or to a $^3\Sigma_u^+$ state or another $^3\Pi_u$ state, both of which can be predicted theoretically to lie within 1 or 2 eV of this energy.

TABLE 4. MOLECULAR-ORBITAL ELECTRON CONFIGURATIONS FOR OXYGEN

Molec.	Electron configuration* state	$3\sigma_g$	$1\pi_u$	$1\pi_g$	$3\sigma_u$	Molec.	Electron configuration* state	$3\sigma_g$	$1\pi_u$	$1\pi_g$	$3\sigma_u$	other
O^-	$X\,^2\Pi_g$	2	4	3	0	O_2^+	$X\,^2\Pi_g$	2	4	1	0	
	$^2\Pi_u$	2	3	4	0		$a\,^4\Pi_u$	2	3	2	0	
O_2	$X\,^3\Sigma_g^-$	2	4	2	0		$A\,^2\Pi_u$	2	3	2	0	
	$a\,^1\Delta_g$	2	4	2	0		$b\,^4\Sigma_g^-$	1	4	2	0	
	$b\,^1\Sigma_g^+$	2	4	2	0		$^2\Sigma_g^+$	1	4	2	0	
	$C\,^3\Delta_u$	2	3	3	0		$^4\Sigma_g^+$	2	3	1	1	
	$A\,^3\Sigma_u^+$	2	3	3	0		$^4\Pi_g$	2	2	3	0	
	$c\,^1\Sigma_u^-$	2	3	3	0		$^2\Delta_g$	1	4	2	0	
	$^3\Pi_g$	1	4	3	0		$^2\Sigma_g^-$	1	4	2	0	
	$^1\Pi_g$	1	4	3	0		$^2\Phi_u$	2	3	2	0	
	$^3\Pi_u$	2	4	1	1		$c\,^4\Sigma_u^-$	2	4	2	0	$-2\sigma_u$
	$^1\Pi_u$	2	4	1	1							
	$^5\Pi_g$	2	3	2	1							
	$B\,^3\Sigma_u^-$	2	3	3	0							
	$^1\Delta_u$	2	3	3	0							
	$^1\Sigma_u^+$	2	3	3	0							

* The footnote to Table 2 also applies here, except that for oxygen the $3\sigma_g$ orbital usually lies below the $1\pi_u$ orbital so it has been listed first.

For the $E\,^3\Sigma_g^+$ state, only approximate (band-head) values of $G(0)$ and $G(1)$ are available, and no rotational constants.[28] However, MULLIKEN's interpretation[13] of this state as the lowest Rydberg state seems firmly founded, and consequently the lower portion of the curve can be obtained simply by moving the $N_2^+ X\,^2\Sigma_g^+$ curves downward (compare, for example, the NO $A\,^2\Sigma^+$ and $NO^+ X\,^1\Sigma^+$ curves, Fig. 2). At some distance above its minimum, the curve probably turns over and joins a nearly-flat $^3\Sigma_g^+$ curve coming from the $^4S^0 + {}^2D^0$ dissociation limit, as indicated in Fig. 1. Very recently JOSHI[39] appears to have found $E^3\Sigma_g^+ \rightarrow A^3\Sigma_u^+$ bands originating from $v = 2$ to 5. If this discovery is confirmed, it means that the E curve must rise considerably higher than shown in Fig. 1 before turning over and descending to the dissociation limit.

Figure 1 includes a curve for the $b'\,{}^1\Sigma_u^+$ state even though the levels above $v = 3$ are irregular and may possibly belong to a different state. The lowest possible dissociation limit for the b' state is $^2D^0 + {}^2P^0$ at 15·75 eV. However, a state of the same type, $j\,{}^1\Sigma_u^+$, is known to lie about 0·35 eV below the b' state.[13,28] Although only one vibrational level of this state has been observed, its measured rotational constant makes it virtually impossible to join its curve into the b' curve to give a single curve with a double minimum (as was done with the C and C' states). Consequently, by the noncrossing rule, the j state will pree-mpt the lowest dissociation limit, and b' will go to the next lowest, $^4S^0 + 3s\,{}^4P$, at 20·09 eV. At intermediate internuclear distances, however, the b' curve will probably behave as if it were approaching the $N^+(^3P) + N^-(^3P)$ dissociation limit at 24·6 eV.[13] This is borne out by the way that an extrapolation of the Rydberg–Klein portion of the curve goes smoothly into a simple Coulomb $N^+ + N^-$ curve, as shown in Fig. 1.

In addition to $b'\,{}^1\Sigma_u^+$, a large number of other states of N_2 above 12 eV have been observed,[13,28,40] and Mulliken has sketched curves for some of them (see WILKINSON[41]). In most cases, however, only a few vibrational levels have been observed, and the vibrational numbering is uncertain. In fact, the recent preliminary investigation of CARROLL and MAHON-SMITH[42] using various isotopes shows that some of the "different" states are probably different vibrational levels of the same state. Because of such uncertainties, these highly-excited states of N_2 have been omitted from the present work.

In addition to the N_2 states discussed above, a large number of repulsive or slightly-attractive states are associated with the dissociation limits $^4S^0 + {}^2D^0$, $^4S^0 + {}^2P^0$, $^2D^0 + {}^2D^0$, and higher limits not shown on Fig. 1. The courses which the curves for these states follow at moderate internuclear distances are not known; hence, only short portions at large internuclear distances are shown on the figures. Because of uncertainties and lack of space, these curves are generally not labeled, and fewer curves are drawn than must actually occur. (The number of molecular states going to the four N + N dissociation limits shown on Fig. 1 are, starting with the lowest, 4, 12, 8 and 30, respectively.)

Some information on such states can be deduced from perturbations and predissociations of the higher known states of N_2. For example, a slightly-repulsive $^3\Sigma_u^+$ state connected with the $^4S^0 + {}^2D^0$ dissociation limit probably predissociates several singlet states, and indirectly the $b'\,{}^1\Sigma_u^+$ state, at around 13 eV.[13,40] However, until further spectroscopic work (especially with isotopes) locates the higher observed N_2 states more accurately, it is difficult to deduce much about the curves of the predissociating states.

If the dissociative recombination of N_2^+ is as rapid as claimed by KASNER, ROGERS and BIONDI,[43] one or more repulsive singlet or triplet N_2 curves should pass near the bottom of the $N_2^+ X\,{}^2\Sigma_g^+$ curve[44] (electron–ion recombination to a quintet or septet state is spin-forbidden). Such a repulsive curve does not go to the $^4S^0 + {}^4S^0$ dissociation limit, and probably not to the $^4S^0 + {}^2D^0$ limit, since the corresponding triplet molecular states probably lie too low. There are several singlet and triplet states belonging to the $^4S^0 + {}^2P^0$ and $^2D^0 + {}^2D^0$ limits which could reasonably lie in the right region, but it does not seem possible at present to reach a more definite conclusion. It should also be mentioned that the recombination-rate measurements could be in error due to impurities, ion clustering, or lack of electron thermalization, especially since the results appear to be contradicted by auroral observations[45] and by the failure to observe N atoms in N_2 bombarded with electrons of energy between 10 and 24 eV[46] (any repulsive N_2 states produced by electron-ion recombination should also be produced by electron bombardment of N_2).

The N_2^+ ion

Potential curves for the observed states of N_2^+, including the recently-discovered $D\ ^2\Pi_g$ state, have been calculated using the numerical Rydberg–Klein method described in Section II. The required spectroscopic data were taken from the references cited by WALLACE,[28] plus additional papers by JANIN and coworkers[47–49] and by TANAKA and coworkers.[50,51] The energies of the N_2^+ states relative to that of ground-state N_2 were obtained from the Worley-Jenkins Rydberg series.[2,28,40] The results for the $D\ ^2\Pi_g$ curve agree within 0·002 Å with the results of NAMIOKA, YOSHINO and TANAKA,[51] while the $B\ ^2\Sigma_u^+$ curve agrees reasonably well with that obtained by GRANDMONTAGNE and EIDO[52] using the original Rydberg–Klein graphical method. (The unusual shape of the $B\ ^2\Sigma^+$ curve was explained plausibly by DOUGLAS[53] as due to interaction with the $C\ ^2\Sigma_u^+$ state; however, Douglas gives a schematic potential curve of incorrect shape.) No previous work is available for comparison with the present calculations for the $X\ ^2\Sigma_g^+$, $A\ ^2\Pi_u$ and $C\ ^2\Sigma_u^+$ curves.

For the $A\ ^2\Pi_u$ state only the vibrational levels up to $v = 9$ have been observed directly, but from perturbations in the $B\ ^2\Sigma_u^+$ state JANIN, D'INCAN and MARCHAND[49] have determined the position of levels up to $v = 28$. These values, when combined with an extrapolation of the inner branch of the $A\ ^2\Pi_u$ curve, permit determination of the outer branch to a relatively high energy.

The $N_2^+ X$, A, B and D curves in Fig. 1 were smoothly extrapolated to their dissociation limit ($^4S^0 + {}^3P$) with some help from a valence-bond relation between the Σ and Π states derived by KNOF, MASON and VANDERSLICE.[54] Curves for the predicted quartet and sextet states going to the same dissociation limit were then obtained, at large internuclear distances, by use of valence-bond relations between these states and the observed doublet states.[54]

The behavior of these states, and others corresponding to higher dissociation limits, at small internuclear distances can be estimated from molecular-orbital theory. MULLIKAN[13] predicted that two of the N_2^+ quartet states would be stable, but, partly on the basis of the valence-bond calculations and on the stability of the new $D\ ^2\Pi_g$ state, the writer believes that several others are also stable. The lowest quartet state should be $^4\Sigma_u^+$, at 21 or 22 eV,[13] with a $^4\Delta_u$ and a $^4\Sigma_u^-$ state lying about 1 and 2 eV above it, respectively (like the N_2 $A\ ^3\Sigma_u^+$, $^3\Delta_u$ and $B'\ ^3\Sigma_u^-$ states; see Table 2).

Some information on N_2^+ states can be deduced from electron-bombardment experiments. In bombardment of nitrogen at not-too-low pressures, several workers have observed the production of N_3^+, probably by the reactions

$$N_2 + e \rightarrow N_2^{+*} + 2e,\ N_2^{+*} + N_2 \rightarrow N_3^+ + N,$$

with a threshold of about 21·04 eV.[55] ČERMÁK and HERMAN[56] found that the variation of the ion current with electron energy (between 21 and 350 eV) corresponds to a forbidden transition,[17] such as the production of N_2^+ in a quartet state. Shortly above the threshold, at 21·9 eV, CURRAN[55] noted that the ion current rises sharply. For this reason, the $^4\Delta_u$ state is shown at 21·9 eV in Fig. 1. If these two energies correspond to the lowest vibrational levels of the two quartet states, the Franck–Condon factors for the (0,0) transitions from the ground state of N_2 are evidently fairly large, so the r_e values of the quartet state are fairly small as shown on Fig. 1. However, such small r_e values seem unlikely for this molecular-orbital configuration (Table 2), so perhaps these states lie

lower and have larger r_e values, so that the first observed transitions are (1,0) or (2,0). The situation is also complicated by possible resonances with the energy levels of N_3^+.

CURRAN[55] also indicated a third threshold at 22·6 eV, but his experimental points actually show a rather smooth variation of ion current in this region, which could be caused by contributions from successively higher vibrational levels. Accordingly, the $^4\Sigma_u^-$ state has been placed slightly higher in Fig. 1, following theoretical expectation.

Above these three quartet states should lie three similar doublet states of the same configuration: $C\,^2\Sigma_u^+$, $^2\Delta_u$, and $^2\Sigma_u^-$ (Table 2). The shape of the $C\,^2\Sigma_u^+$ curve, however, is different from that of the other five curves, because of "interaction" between the $B\,^2\Sigma_u^+$ and $C\,^2\Sigma_u^+$ states.[53] More precisely, at small internuclear distances the electron configuration of the C state is similar to that of the other five states; at slightly larger distances the configuration shifts toward one with a missing $2s$ electron; while at still larger distances, approaching the dissociation limit, another shift must occur if the non-crossing rule is obeyed. Thus, it is not surprising that the extrapolated portion of the C curve shows a potential maximum (actually, the maximum might be considerably higher than shown in Fig. 1).

An upper limit for the position of the $^2\Sigma_u^-$ state is placed by its perturbation of the $v = 3$ level of the $C\,^2\Sigma_u^+$ state.[57] The $^2\Delta_u$ state should lie somewhat below the $^2\Sigma_u^-$ state; probably its higher levels perturb the $v = 2$ and 6 levels of the C state.[57] The curves for these two doublet states have been drawn with r_e values estimated from their electron configuration. The values are not consistent with those used for the quartet states of the same configuration; perhaps the curves for the quartet states are incorrect, as discussed above.

Figure 1 also shows approximate curves for three other N_2^+ quartet states, $^4\Pi_g$, $^4\Pi_u$, and $^4\Sigma_g^+$, that are probably slightly stable, based on valence-bond[54] and molecular-orbital considerations (Table 2), plus the evidence that the $^4\Pi_u$ state predissociates the $C\,^2\Sigma_u^+$ state at $v = 3$.[57]

A study of the N_2^+ curves in Fig. 1 indicates the possible occurrence of several permitted band systems which have not yet been identified in spectroscopic studies, specifically, $D\,^2\Pi_g \rightarrow B\,^2\Sigma_u^+$; $^4\Pi_g \rightarrow (^4\Sigma_u^+, {}^4\Delta_u, {}^4\Sigma_u^-)$; and $(^2\Sigma_u^-, {}^2\Delta_u, C\,^2\Sigma_u^+) \rightarrow D\,^2\Pi_g$. It is tempting to try to correlate these with some of the observed but unidentified band systems of nitrogen. Some time ago, when the writer believed that the $^4\Delta_u$ and $^4\Sigma_u^-$ states were considerably higher and the $^4\Pi_g$ state considerably lower than now indicated, he suggested in private communications that Gaydon's green system[28,40] could be a $^4\Delta_u \rightarrow {}^4\Pi_g$ or $^4\Sigma_u^- \rightarrow {}^4\Pi_g$ transition. However, with the revised positions, this interpretation is no longer reasonable, and the stronger quartet bands should lie in the infrared. It is possible that the HEPNER–HERMAN infrared bands[37] represent the $N_2^+\ {}^4\Pi_g \rightarrow {}^4\Sigma_u^+$ transition. Gaydon's green bands fit the $^2\Delta_u \rightarrow D\ {}^2\Pi_g$ transition quite well using only the levels $v'' \geqslant 6$, but it would be very strange that bands going to the $v'' = 0$ to 5 levels are not observed in the blue spectral region. The vibrational intervals of the upper state of Herman's near-infrared system[28,40] agree very well with those of the $D\,^2\Pi_g$ state, but the levels of the lower state do not agree with either the $A\,^2\Pi_u$ or the $B\,^2\Sigma_u^+$ levels (or any combination of the two). Moreover, the bands are degraded the wrong way for such transitions. Even after considerable study, the writer has found no very convincing arguments for making new N_2^+ identifications.

The N_2^{++} *ion*

Although states of the N_2^{++} ion are too high to be shown in Fig. 1 (the lowest lies at about 42 eV), they have been observed in mass spectrometers, and one electronic transition has been observed spectroscopically.[58] HURLEY[59] has calculated potential energy curves for seven of the more-stable electronic states, with the help of data from isoelectronic neutral molecules. Although all of the states are unstable against dissociation into $N^+ + N^+$, many of them have potential maxima (at intermediate internuclear distances) sufficiently high to give them lifetimes of many seconds. For further details of the potential curves, the reader is referred to the paper by HURLEY.[59]

The NO^- *ion*

Since this negative ion has been observed in mass spectrometers,[60] and existence of a metastable state is quite unlikely theoretically, its ground state is probably stable (i.e. has a positive electron affinity). It should be similar to the $X\ ^3\Sigma_g^-$ state of the isoelectronic O_2 molecule, with a dissociation energy of about 5 eV. Its dissociation limit lies 5·04 eV above the ground state of NO (see Section IV), so its minimum probably lies only a fraction of a volt below that of the NO $X\,^2\Pi$ state. The $NO^- X\,^3\Sigma^-$ curve in Fig. 2 has been drawn accordingly, using the corresponding O_2 curve as a guide.

Predicted repulsive NO^- states going to the lowest dissociation limit are also indicated on Fig. 2, but not extended very far. Probably the $^3\Pi$ state is the intermediate state involved in the production of $N + O^-$ when NO is bombarded by electrons, so that its curve at smaller internuclear distances corresponds to the curve deduced by CLOUTIER and SCHIFF[61] from electron-impact data.

The NO *molecule*

Spectroscopic data used to calculate Rydberg–Klein curves for the observed states of NO were obtained from the references listed by WALLACE,[28] with the addition of work by THOMPSON and GREEN,[62] MIESCHER,[63] and HUBER and MIESCHER.[64] The results agree with the less-complete results of VANDERSLICE, MASON and MAISCH[8] to within 0·004 Å.

Although transitions involving the predicted quartet states of NO have not been identified with certainty by fine-structure analysis, it is highly probable that the near-infrared bands observed by OGAWA[65] and BROOK and KAPLAN[66] represent the $b\,^4\Sigma^- \rightarrow a\,^4\Pi$ transition. If the two states have about the same r_e values as the corresponding states of O_2^+ (see Fig. 3), the relative intensities of the bands (insofar as they can be estimated from the published papers) agree with theory, provided that Brook and Kaplan's vibrational numbering for the $^4\Sigma^-$ state is increased by one. (The unobserved bands corresponding to $v' = 0$ will then lie mostly in the little-investigated region beyond 11,000 Å.) When the energy of the $^4\Pi$ state is derived from the M bands ($a\,^4\Pi \rightarrow X\,^2\Pi$) of NO in a frozen argon matrix,[67] and the two quartet curves are drawn by analogy with the corresponding O_2^+ curves, they intersect at about the $^4\Pi$ dissociation limit, which lies slightly above the $v = 4$ level of the $^4\Sigma^-$ state (see Fig. 2). The failure to observe bands originating from $v > 4$ can thus be easily explained as due to predissociation of the $^4\Sigma^-$ state by the $^4\Pi$ state.

At large internuclear distances, curves for all the NO states going to the lowest dissociation limit of NO were obtained from the valence-bond calculations of MEADOR,[30] which appear to be more accurate than those of VANDERSLICE, MASON and MAISCH.[8] These

calculations do not yield a loosely-bound state, such as postulated by BARTH, SCHADE and KAPLAN[68] to explain details of the nitric-oxide afterglow. However, the arguments of the latter are not conclusive because the radiative lifetimes of the $A\,^2\Sigma^+$ and $B\,^2\Pi$ states are about two orders of magnitude longer than they assumed, since the f-values for the γ and β bands are quite small.[69]

It has often been suggested that the $^2\Sigma^+$ curve going to the lowest dissociation limit should be nearly flat, in order to explain, by predissociation, the failure to observe emission from the higher vibrational levels of the $B\,^2\Pi$ and $C\,^2\Pi$ states. However, the weakness of the predissociation (no line broadening is observed in absorption[70]), and certain features of afterglow emission,[71] are much better explained as a predissociation by the $a^4\Pi$ state. Moreover, quantum-mechanical calculations[72] put the lowest non-Rydberg $^2\Sigma^+$ state 2 or 3 eV higher, where it could intersect the $M\,^2\Sigma^+$ curve and explain the observed diffuseness[63] of the $v = 2$ level of this state. Such a non-Rydberg $^2\Sigma^+$ curve would cross the $A\,^2\Sigma^+$, $D^2\,\Sigma^+$, $E\,^2\Sigma^+$, $H\,^2\Sigma^+$, and $M\,^2\Sigma^+$ Rydberg curves. By the non-crossing rule, electronic interactions will prevent such crossings, but if the interaction parameter is small the curves will look almost as if they cross, as shown in Fig. 2. A molecule in the $M\,^2\Sigma^+$, $v = 2$, level can still predissociate by following the repulsive $^2\Sigma^+$ curve(s), "jumping across" the small gaps because of a breakdown of the Born–Oppenheimer approximation (which approximation implies that a molecule must follow a particular potential curve based on an electronic energy independent of the relative velocity of the nuclei). The same repulsive $^2\Sigma^+$ curve is probably followed when an NO^+ ion dissociatively recombines with an electron.

TANAKA and SAI[28,73] have claimed to observe $A\,^2\Sigma^+$ levels up to $v = 15$, and $D\,^2\Sigma^+$ levels up to $v = 11$. This observation is inconsistent with the A and D curves shown in Fig. 2. However, Tanaka and Sai did not make a fine structure analysis, and it seems likely that they were observing levels of the higher $^2\Sigma^+$ states (E, H, M, etc.) instead.

From the underlying absorption continuum of NO, MARMO[74] has deduced a repulsive portion of a $^2\Sigma^+$ curve in the 9 to 10 eV region and extrapolated it to the lowest dissociation limit of NO. However, his curve seems too high to explain the observed diffuseness of $M^2\,\Sigma^+$, $v = 2$. More likely it belongs to the second lowest non-Rydberg $^2\Sigma^+$ state, which goes to the $^2D^0 + {}^3P$ dissociation limit. This $^2\Sigma^+$ state, which is expected from molecular-orbital considerations (Table 3) to be loosely bound, fits in reasonably well with Marmo's curve, as shown in Fig. 2.

In agreement with the non-crossing rule, the $B\,^2\Pi$ and $C\,^2\Pi$ states of NO are shown to share a single potential curve with a double minimum. Before this curve can be regarded as established, however, it should be demonstrated that the irregularly-spaced ("perturbed") higher levels of these states agree with the eigenvalues for this single curve.

A stable $^2\Phi$ state is predicted for NO, though it has never been observed. MULLIKEN[12] placed it slightly below the $B\,^2\Pi$ state, probably because, among states of the same molecular-orbital configuration and multiplicity (Table 3), those with the largest angular momentum usually lie lowest. However, this particular configuration includes three $^2\Pi$ states, and it seems not unreasonable that interactions could cause the lowest of these (i.e. $B\,^2\Pi$) to lie considerably below the $^2\Phi$. This would explain why HUBER, HUBER and MIESCHER[75] have not found $B'\,^2\Delta \rightarrow {}^2\Phi$ bands, even after looking carefully for them. (Transitions between the $^2\Phi$ state and almost all other NO states are forbidden.) The $^2\Phi$ curve on Fig. 2 has been drawn accordingly.

The $B'\,^2\Delta$ and $G\,^2\Sigma^-$ curves shown on Fig. 2 were calculated from published data[63] and extrapolated monotonically to their dissociation limit. However, LOFTUS and MIESCHER[76] have very recently observed several additional vibrational levels of these states, and these levels tend toward limits higher than the $^2D^0+^3P$ dissociation limit. Accordingly, the B' and G curves in Fig. 2 should probably be shown with potential maxima at around 2 Å.

Short sections of other molecular curves going to the five lowest dissociation limits of NO are shown in Fig. 2. However, only a few of the 18 curves going to the $^2D^0+^3P$ limit, and the 12 curves going to the $^2P^0+^3P$ limit, are indicated. It is interesting to note that the limits involving $O(^1D)$ and $O(^1S)$ (the upper states of the red and green airglow lines) correspond only to quartet states, so that production of such excited oxygen atoms by dissociative recombination of NO^+ or photo-dissociation of NO is spin-forbidden, except at considerably higher energies, corresponding to dissociation limits not shown on Fig. 2.

The NO^+ *ion*

The potential curves for the $X\,^1\Sigma^+$ and $A\,^1\Pi$ states of NO^+ shown in Fig. 2 are based on Rydberg–Klein calculations, using published spectroscopic data,[28,77] with smooth extrapolations to the dissociation limits. Since rotational data are available only for five of the levels of the X state and two of the levels of the A state, the upper portions of these curves are somewhat uncertain.

No bands connecting other states of NO^+ have been analyzed. However, HUBER[78] has recently reinvestigated Tanaka's three Rydberg series in NO, which converge to three excited states of NO^+. Huber gives fairly convincing arguments for believing that the lowest of these series limits, at 14·22 eV, corresponds to a $^3\Sigma^+$ state. The second, at 16·56 eV, could be a $^3\Pi$ or a $^3\Delta$ state, but probably the latter, since transitions between it and the $^3\Sigma^+$ state have not been observed. The $^3\Sigma^+$ and $^3\Delta$ curves in Fig. 2 are based on these series limits, together with knowledge of the number of vibrational levels observed in the Rydberg series, which enables estimation of the r_e values (using the Franck–Condon principle). However, one would predict considerably larger r_e values from the electron configuration (Table 3; also cf. the $^3\Sigma^-$ state, discussed below). This discrepancy could be explained if all the observed Rydberg series correspond to excited vibrational levels. If true, the $^3\Sigma^+$ and $^3\Delta$ curves in Fig. 2 should be adjusted downward and to the right.

Tanaka's highest Rydberg limit, at 18·33 eV, corresponds to the observed $A\,^1\Pi$ state.[78] Data for this limit, when combined with data from the $A\rightarrow X$ bands, give an accurate value for the ionization energy of NO: $74{,}746 \pm 40\ cm^{-1} = 9{\cdot}267 \pm 0{\cdot}005$ eV.[78]

In addition to these NO^+ states, a $^3\Pi$ state should lie somewhat below the $A\,^1\Pi$ state. It is quite surprising that $^3\Pi\rightarrow{}^3\Sigma^+$ bands of NO^+ have never been identified, since the corresponding bands in the isoelectronic molecules N_2 (first positive bands) and CO (Asundi bands) are prominent in nitrogen and carbon monoxide discharges. However, ZAPESOCHNY, *et al.*[79] mention "a band of NO^+ (electronic transition unknown, $\lambda = 4380$ Å)", with no further details. The $^3\Pi$ curve in Fig. 2 has been somewhat arbitrarily drawn as if this band were the $^3\Pi\rightarrow{}^3\Sigma^+$ (0,0) transition. Although this assumption may be wrong, the $^3\Pi$ position indicated is unlikely to be in error by more than an electron volt. The r_e value has been chosen so that no particular vibrational level is likely to stand

out in a Rydberg series, thus explaining the failure of Tanaka and Huber to pick out such a series.

From perturbations of the $A\,^1\Pi$ state MIESCHER[77] deduced the energy and rotational constant of one level of a $^3\Sigma^-$ state. The $^3\Sigma^-$ curve in Fig. 2 is drawn under the assumption that this level is the lowest vibrational level, although it could be a higher level; thus, the $^3\Sigma^-$ curve could lie somewhat lower. Similar $^1\Sigma^-$ and $^1\Delta$ curves (see Table 3) have been added above the $^3\Sigma^-$, by analogy with N_2 (Fig. 1) and CO. The $^5\Sigma^+$ and $^7\Sigma^+$ curves have also been copied from N_2, and short portions of some of the curves going to the second dissociation limit have been indicated.

The NO^{++} *ion*

Although this metastable ion has not been identified by optical spectroscopy, it has been observed in mass spectrometers, with an appearance potential in NO of about 40 eV.[59] Theoretical curves for three of its electronic states have been obtained by HURLEY;[59] they are too high to be shown in Fig. 2.

The O_2^- *ion*

That O_2^- is stable has been known for a long time, but quantitative estimates of its stability have differed considerably. Recently, PHELPS and PACK[80,81] measured electron attachment and detachment rates in oxygen, from which they calculated an electron affinity of $0{\cdot}44 \pm 0{\cdot}02$ eV. Later, CURRAN[82] obtained a lower limit of 0·58 eV, based on the appearance potential of O_2^- in electron-bombarded O_3. The disagreement could be due to production of vibrationally excited O_2^- by Phelps and Pack (although their results were unchanged even after the O_2^- ions collided 5×10^8 times with O_2 molecules), or to some unknown source of error in their work or in that of Curran. Since theoretical considerations suggest a still smaller value ($\sim 0{\cdot}2$ eV) for the electron affinity,[83] the value of 0·44 eV represents a reasonable compromise which probably lies within 0·2 eV of the true value.

The electron affinity gives the energy of the ground state of O_2^-, which theory shows must be a $^2\Pi_g$ state.[83,84] X-ray data on KO_2 crystals show that the r_e value of O_2^- is about 1·30 Å, while the fluorescence spectrum of O_2^- dispersed in alkali halide crystals gives a vibrational spacing of about 0·14 eV.[85] The $X\,^2\Pi_g$ curve in Fig. 3 has been drawn accordingly.

It has been suggested that the lowest excited state of O_2^- is a Rydberg $^4\Sigma_g^-$ state.[84] However, such a state probably does not exist because the Rydberg orbital is not bound.[83] Accordingly, such a curve has not been included in Fig. 3.

Excited non-Rydberg states of O_2^- have been discussed by MASSEY,[84] but a comparison with recent quantum-mechanical calculations for the isoelectronic F_2^+ ion,[14,86] and with data on excited states of O_2,[83] shows that the $^4\Sigma_u^-$ and $^2\Delta_u$ states probably lie considerably higher than Massey suggests, while a $^2\Sigma_g^+$ and a $^2\Pi_u$ state lie below them. The O_2^- fluorescence observed by ROLFE[85] very likely corresponds to the $^2\Pi_u \rightarrow X\,^2\Pi_g$ transition; this interpretation puts the $^2\Pi_u$ state about 3·65 eV above the ground state of O_2^-. A portion of the $^2\Pi_u$ curve is sketched on Fig. 3. Others of the twenty-four O_2^- states going to the lowest dissociation limit are merely indicated by a few short, dotted curves. Two of these states, $^4\Sigma_u^-$ and $^2\Sigma_u^-$, may be formed by the simple addition of an electron to the ground state of O_2; hence, the well-known electron-bombardment reaction, $O_2 + e \rightarrow O^- + O$, probably takes place via these repulsive states.

The O_2 molecule

Rydberg–Klein curves for the observed states of O_2 were calculated using spectroscopic data from the references listed by WALLACE.[28] The results agree with the less-complete results of VANDERSLICE, MASON and MAISCH[9] to within 0·002 Å except for three states: for the $c\,^1\Sigma_u^-$ state their results appear to contain a numerical error; for the $B\,^3\Sigma_u^-$ state differences up to 0·005 Å occur due to the present writer's smoothing of the irregular observed B_v values; and for the A and B states differences up to 0·051 Å occur for the highest vibrational levels (near the dissociation limit) due to the sensitivity of the results in this region to small variations in method and input data.

In Fig. 3 the right-hand portions of most of the eighteen O_2 curves going to the lowest dissociation limit ($^3P+^3P$) have been taken from the valence-bond calculations of VANDERSLICE, MASON and MAISCH,[9] but the $^3\Pi_g$, $^1\Pi_g$ and $^1\Sigma_g^+$ curves have been lowered because these states will interact with other low-energy electronic configurations not considered in the simple valence-bond treatment. The $^3\Pi_u$ curve has been extended to intersect the left branch of the $B\,^3\Sigma_u^-$ curve at $v = 4$, in order to explain the predissociation results of CARROLL.[87] The upper portion of the left branch of the $B\,^3\Sigma_u^-$ curve has been taken from the work of EVANS and SCHEXNAYDER,[88] based on the variation with wavelength of the Schumann–Runge absorption continuum.

Curves for two high-energy O_2 states, $^1\Delta_u$ and $^1\Sigma_u^+$, have been sketched in Fig. 3 by assuming that their energies, above that of the $B\,^3\Sigma_u^-$ state, vary smoothly with internuclear distance from the values (2·8 and 5·6 eV, respectively) calculated by ITOH and OHNO[89] quantum-mechanically at 1·207 Å, to the known values (2·0 and 4·2 eV) at the dissociation limits.

The many other O_2 states going to the higher dissociation limits are indicated in Fig. 3 by a few short, dashed curves.

In ultraviolet absorption spectroscopy a number of excited states of O_2 above 9·6 eV have been observed,[28] but no identifications or rotational analyses have been made. These states are probably all Rydberg states, containing an outer electron loosely bound to an O_2^+ core. The lowest Rydberg state is expected to be a $^3\Pi_g$ state at about 8 eV; it would not be observed in absorption because transitions between it and the ground state are forbidden. Its curve may well have a peculiar shape because of interaction with the $^3\Pi_g$ curve coming from the lowest dissociation limit. Because of this and other complications, no curves for Rydberg states have been included in Fig. 3.

The O_2^+ ion

Rydberg–Klein calculations were made for the four well-known states of O_2^+ using spectroscopic data from the work referenced by WALLACE[28] and recent papers by WENIGER[90] and LE BLANC.[91] The energies of these states relative to O_2 are fixed by WATANABE and MARMO's photoionization threshold[92] and TANAKA and TAKAMINE's first Rydberg series.[93] The approximate valence-bond relations of KNOF, MASON and VANDERSLICE[54] were used to assist in extrapolation of the X, a and A curves to their dissociation limit, as well as to estimate the outer portion of all other curves going to the lowest dissociation limit. The results are shown in Fig. 3.

By the simple removal of one valence-shell electron (Table 4) from the ground state of O_2 precisely five states of O_2^+ can be formed: the well-known X, a, A and b states, and a not-yet-identified $^2\Sigma_g^-$ state analogous to the G state of NO (see Fig. 2). It is quite

probable that the $^2\Sigma_g^-$ state corresponds to the limit of TANAKA and TAKAMINE's second Rydberg series,[93] since the appearance, energy, and vibrational spacing all agree with predictions. The curve for this state is shown accordingly in Fig. 3.

Two other stable O_2^+ states in this region can be predicted: $^2\Delta_g$ and $^2\Phi_u$ (cf. NO, Fig. 2). Estimates of their position are presented in Fig. 3.

Removal of one $2\sigma_u$ electron from the ground state of O_2 should produce two stable states: $c\,^4\Sigma_u^-$ and $^2\Sigma_u^-$. The former has recently been identified by LE BLANC[91] as the upper state of Hopfield's emission bands, and very recently CODLING[94] has discovered Rydberg series converging to its two lowest vibrational levels. The corresponding doublet state is as yet unobserved; it probably lies 1 or 2 eV above the quartet state.

The O_2^{++} ion

Although this metastable ion has not been identified by optical spectroscopy, it has been observed in mass spectrometers, with an appearance potential in O_2 of about 36 eV.[95] Theoretical curves for eight of its electronic states have been obtained by HURLEY;[59] they are too high to be shown in Fig. 3.

Acknowledgements—The writer gratefully acknowledges helpful discussions and correspondence with R. S. MULLIKEN, P. K. CARROLL, Y. TANAKA, K. C. JOSHI, D. BRIGLIA, J. W. MCGOWAN, and R. L. PLATZMAN; and useful communications from E. MIESCHER, A. LOFTHUS, J. T. VANDERSLICE, E. A. MASON, V. ČERMÁK, Z. HERMAN, and K. CODLING. He especially thanks Professor MULLIKEN for a critical reading of the original manuscript.

REFERENCES

1. P. M. MORSE, *Phys. Rev.* **34**, 57 (1929).
2. G. HERZBERG, *Spectra of Diatomic Molecules*, 2nd ed., Van Nostrand Company, Inc., New York. 1950.
3. J. T. VANDERSLICE, E. A. MASON and W. G. MAISCH, *J. Mol. Spectrosc.* **3**, 17 (1959); errata **5**, 83 (1960).
4. R. RYDBERG, *Z. Phys.* **73**, 376 (1931).
5. O. KLEIN, *Z. Phys.* **76**, 226 (1932).
6. A. L. G. REES, *Proc. Phys. Soc. (London)*, **59**, 998 (1947).
7. J. T. VANDERSLICE, E. A. MASON and E. R. LIPPINCOTT, *J. Chem. Phys.* **30**, 129 (1959).
8. J. T. VANDERSLICE, E. A. MASON and W. G. MAISCH, *J. Chem. Phys.* **31**, 738 (1959).
9. J. T. VANDERSLICE, E. A. MASON and W. G. MAISCH, *J. Chem. Phys.* **32**, 515 (1960); errata **33**, 614 (1960).
10. W. R. JARMAIN, *Canad. J. Phys.* **38**, 217 (1960).
11. W. R. JARMAIN, Transition Probabilities of Molecular Band Systems, XVII: Tabulated Klein–Dunham Potential Energy Functions for Fifteen States of N_2, N_2^+, NO, O_2, C_2, and OH, Univ. of Western Ontario, *GRD-TN*-60-498, July 1, 1960.
12. R. S. MULLIKEN, *Rev. Mod. Phys.* **4**, 1 (1932).
13. R. S. MULLIKEN, *The Threshold of Space*, p. 169, (M. ZELIKOFF ed.), Pergamon Press, New York (1957).
14. S. FRAGA and B. J. RANSIL, *J. Chem. Phys.* **35**, 669 (1961).
15. J. W. RICHARDSON, *J. Chem. Phys.* **35**, 1829 (1961).
16. R. S. MULLIKEN, *J. Chem. Phys.* **37**, 809 (1962).
17. J. D. CRAGGS and H. S. W. MASSEY, *Handbuch der Physik*, Springer-Verlag, Berlin, **37**/1, 314 (1959).
18. L. BREWER and A. W. SEARCY, *Ann. Rev. Phys. Chem.*, Vol. 7, 1956, p. 259.
19. NAS-NRC Committee on Fundamental Constants, *Physics Today*, **17**, 48 (1964).

20. P. BRIX and G. HERZBERG, *Canad. J. Phys.* **32**, 110 (1954).
21. Joint Army–Navy–Air Force Thermochemical Panel, *JANAF Thermochemical Tables*, Supplement No. 10, June 30 (1963).
22. C. E. MOORE, *Atomic Energy Levels*, Nat. Bur. Stand. Circular 467, June 15 (1949).
23. E. CLEMENTI and A. D. MCLEAN, *Phys. Rev.* **133**, A419 (1964).
24. L. M. BRANSCOMB, *et al.*, *Phys. Rev.* **111**, 504 (1958).
25. A. G. GAYDON, *Dissociation Energies and Spectra of Diatomic Molecules*, Chapman and Hall, London (1953).
26. G. J. SCHULZ, *Phys. Rev.* **125**, 229 (1962).
27. D. R. BATES, *Mon. Not. R. Astr. Soc.* **112**, 614 (1952).
28. L. WALLACE, *Astrophys. J. Suppl.*, Vol. 7, 165 (1962).
29. Y. TANAKA, M. OGAWA and A. S. JURSA, *J. Chem. Phys.* **40**, 3690 (1964).
30. W. E. MEADOR, Jr., *The Interactions Between Nitrogen and Oxygen Molecules, NASA TR R-68* (1960).
31. P. K. CARROLL, *J. Chem. Phys.*, **37**, 805 (1962).
32. C. KENTY, *J. Chem. Phys.* **35**, 2267 (1961); and **37**, 1567 (1962).
33. A. B. KING and C. GATZ, *J. Chem. Phys.* **37**, 1566 (1962).
34. P. K. CARROLL, *Proc. Roy. Soc. (London)*, **272**, 270 (1963).
35. G. BÜTTENBENDER and G. HERZBERG, *Ann. Phys.* **21**, 577 (1935).
36. A. LOFTHUS, *Canad. J. Phys.* **35**, 216 (1957).
37. G. HEPNER and L. HERMAN, *Ann. Geophys.* **13**, 242 (1957).
38. E. R. DAVIDSON, *J. Chem. Phys.* **35**, 1189 (1961).
39. K. C. JOSHI, Air Force Cambridge Research Center, private communication (March 1964).
40. A. LOFTHUS, *The Molecular Spectrum of Nitrogen*, Physics Dept., Univ. of Oslo, Spectroscopic Report No. 2, Dec. 1960.
41. P. G. WILKINSON, *J. Mol. Spectrosc.* **6**, 1 (1961).
42. P. K. CARROLL and D. MAHON-SMITH, *J. Chem. Phys.* **39**, 237 (1963).
43. W. H. KASNER, W. A. ROGERS and M. A. BIONDI, *Phys. Rev. Letters*, **7**, 321 (1961).
44. D. R. BATES and A. DALGARNO, Electronic recombination, in (D. R. BATES, ed.) *Atomic and Molecular Processes*, p. 262, Academic Press, New York (1962).
45. H. H. BRÖMER and U. STILLE, *Optik*, **15**, 382 (1958).
46. D. BRIGLIA, Mass Spectrometer Studies of Ionization Processes in Nitrogen, Physics Dept., Univ. of Calif. at Los Angeles, *AFCRL-64-259*, 1964.
47. J. JANIN, J. D'INCAN and A. ROUX, *Ann. Univ. Lyon, Sci.* **10B**, 7 (1957).
48. J. JANIN and J. D'INCAN, *Rev. Univ. Mines*, **15**, 258 (1959).
49. J. JANIN, J. D'INCAN and J. MARCHAND, *Ann. Univ. Lyon, Sci.* **12B**, 29 (1959).
50. Y. TANAKA, T. NAMIOKA and A. S. JURSA, *Canad. J. Phys.* **39**, 1138 (1961).
51. T. NAMIOKA, K. YOSHINO and Y. TANAKA, *J. Chem. Phys.* **39**, 2629 (1963).
52. R. GRANDMONTAGNE and R. EIDO, *C.R. Acad. Sci., Paris*, **249**, 366 (1959).
53. A. E. DOUGLAS, *Canad. J. Phys.* **30**, 302 (1952).
54. H. KNOF, E. A. MASON and J. T. VANDERSLICE, *J. Chem. Phys.* **40**, 3548 (1964).
55. R. K. CURRAN, *J. Chem. Phys.* **38**, 2974 (1963).
56. V. ČERMÁK and Z. HERMAN, *Coll. Czech. Chem. Comm.* **27**, 1493 (1962).
57. P. K. CARROLL, *Canad. J. Phys.* **37**, 880 (1959).
58. P. K. CARROLL and A. C. HURLEY, *J. Chem. Phys.* **35**, 2247 (1961).
59. A. C. HURLEY, *J. Mol. Spectrosc.* **9**, 18 (1962).
60. P. S. RUDOLPH, C. E. MELTON and G. M. BEGUN, *J. Chem. Phys.* **30**, 588 (1959).
61. G. G. CLOUTIER and H. I. SCHIFF, *J. Chem. Phys.* **31**, 793 (1959).
62. H. W. THOMPSON and B. A. GREEN, *Spectrochim. Acta*, **8**, 129 (1956).
63. E. MIESCHER, *JQSRT* **2**, 421 (1962).
64. K. P. HUBER and E. MIESCHER, *Helv. Phys. Acta*, **36**, 257 (1963).
65. M. OGAWA, *Sci. of Light*, **3**, 39 (1954).
66. M. BROOK and J. KAPLAN, *Phys. Rev.* **96**, 1540 (1954).
67. H. P. BROIDA and M. PEYRON, *J. Chem. Phys.* **32**, 1068 (1960).
68. C. A. BARTH, W. J. SCHADE and J. KAPLAN, *J. Chem. Phys.* **30**, 347 (1959).
69. G. W. BETHKE, *J. Chem. Phys.* **31**, 662 (1959).
70. A. LAGERQVIST and E. MIESCHER, *Helv. Phys. Acta*, **31**, 221 (1958).
71. R. A. YOUNG and R. L. SHARPLESS, *Disc. Faraday Soc.* No. 33, 228 (1962).
72. H. BRION, C. MOSER and M. YAMAZAKI, *J. Chem. Phys.* **30**, 673 (1959).
73. Y. TANAKA and T. SAI, *Sci. Light*, **1**, 85 (1951).

74. F. F. MARMO, unpublished work, quoted in P. J. NAWROCKI and R. PAPA, *Atmospheric Processes*, Geophysics Corporation of America, Report *AFCRL*-595, August 1961.
75. K. P. HUBER, M. HUBER and E. MIESCHER, *Phys. Letters*, **3**, 315 (1963).
76. A. LOFTHUS, University of Oslo, priv. commun. (January 1964).
77. E. MIESCHER, *Helv. Phys. Acta*, **29**, 135 (1956).
78. K. P. HUBER, *Helv. Phys. Acta*, **34**, 929 (1961).
79. I. P. ZAPESOCHNY, *et al.*, *Ukrayin. fiz. zh.* **6**, 770 (1961).
80. A. V. PHELPS and J. L. PACK, *Phys. Rev. Letters*, **6**, 111 (1961),
81. L. M. CHANIN, A. V. PHELPS and M. A. BIONDI, *Phys. Rev.* **128**, 219 (1962).
82. R. K. CURRAN, *J. Chem. Phys.* **35**, 1849 (1961).
83. R. S. MULLIKEN, *Phys. Rev.* **115**, 1225 (1959).
84. H. S. W. MASSEY, *Negative ions* (2nd ed.) Cambridge Univ. Press (1950).
85. J. ROLFE, *J. Chem. Phys.* **40**, 1664 (1964).
86. K. HIJIKATA, *J. Chem. Phys.* **34**, 231 (1961).
87. P. K. CARROLL, *Astrophys. J.* **129**, 794 (1959).
88. J. S. EVANS and C. J. SCHEXNAYDER, Jr., An Investigation of the Effect of High Temperature on the Schumann–Runge Ultraviolet Absorption Continuum of Oxygen, *NASA-TR*-92, 1961.
89. T. ITOH and K. OHNO, *J. Chem. Phys.* **25**, 1098 (1956).
90. S. WENIGER, *J. phys. radium* **23**, 225 (1962).
91. F. J. LE BLANC, *J. Chem. Phys.* **38**, 487 (1963).
92. K. WATANABE and F. F. MARMO, *J. Chem. Phys.* **25**, 965 (1956).
93. Y. TANAKA and T. TAKAMINE, *Sci. Papers Inst. Phys. Chem. Res., Tokyo*, **39**, 437 (1942).
94. K. CODLING, National Bureau of Standards, priv. commun. (April 1964).
95. F. H. DORMAN and J. D. MORRISON, *J. Chem. Phys.* **39**, 1906 (1963).

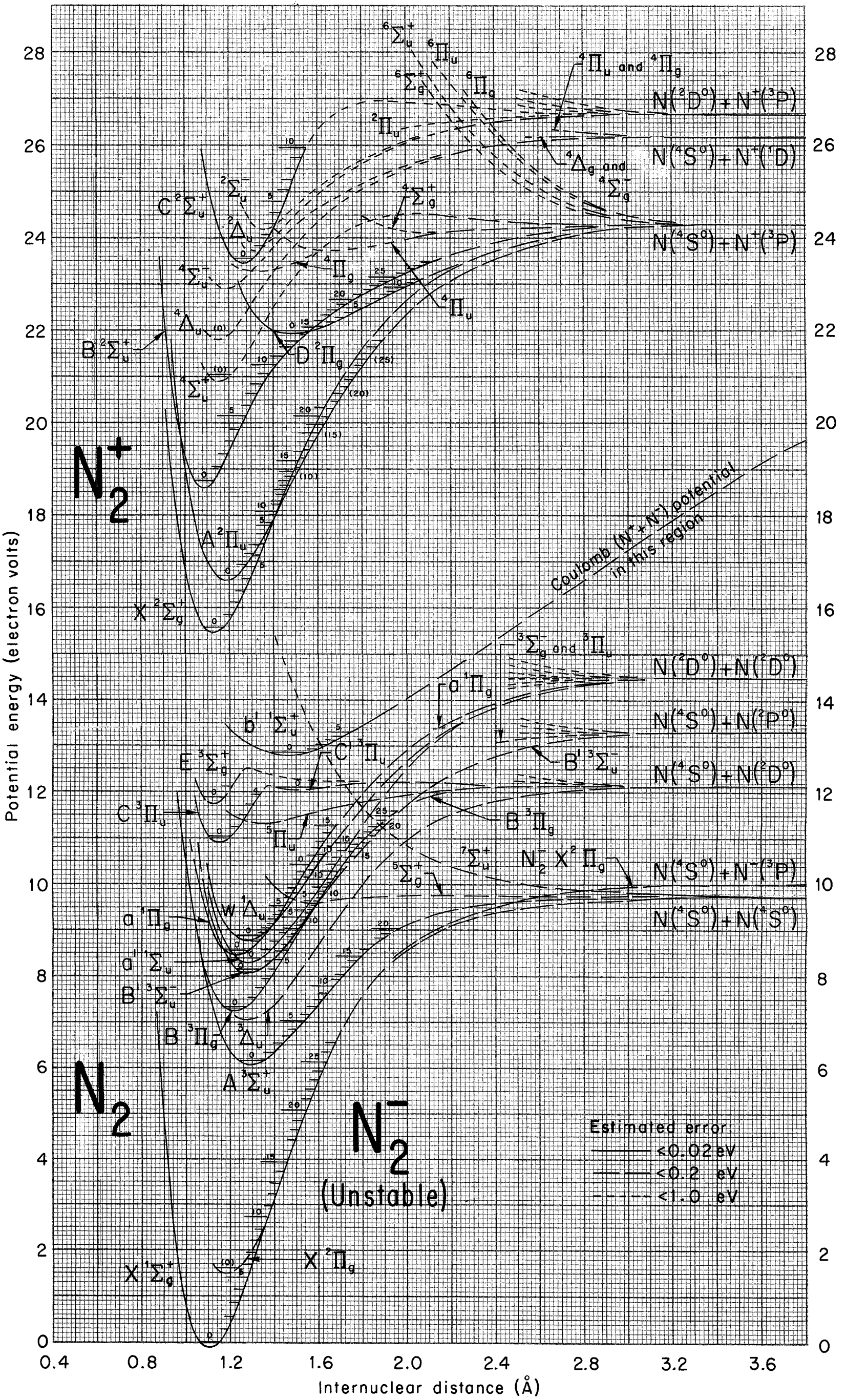

Fig. 1—Potential-energy curves for N_2^- (unstable), N_2 and N_2^+

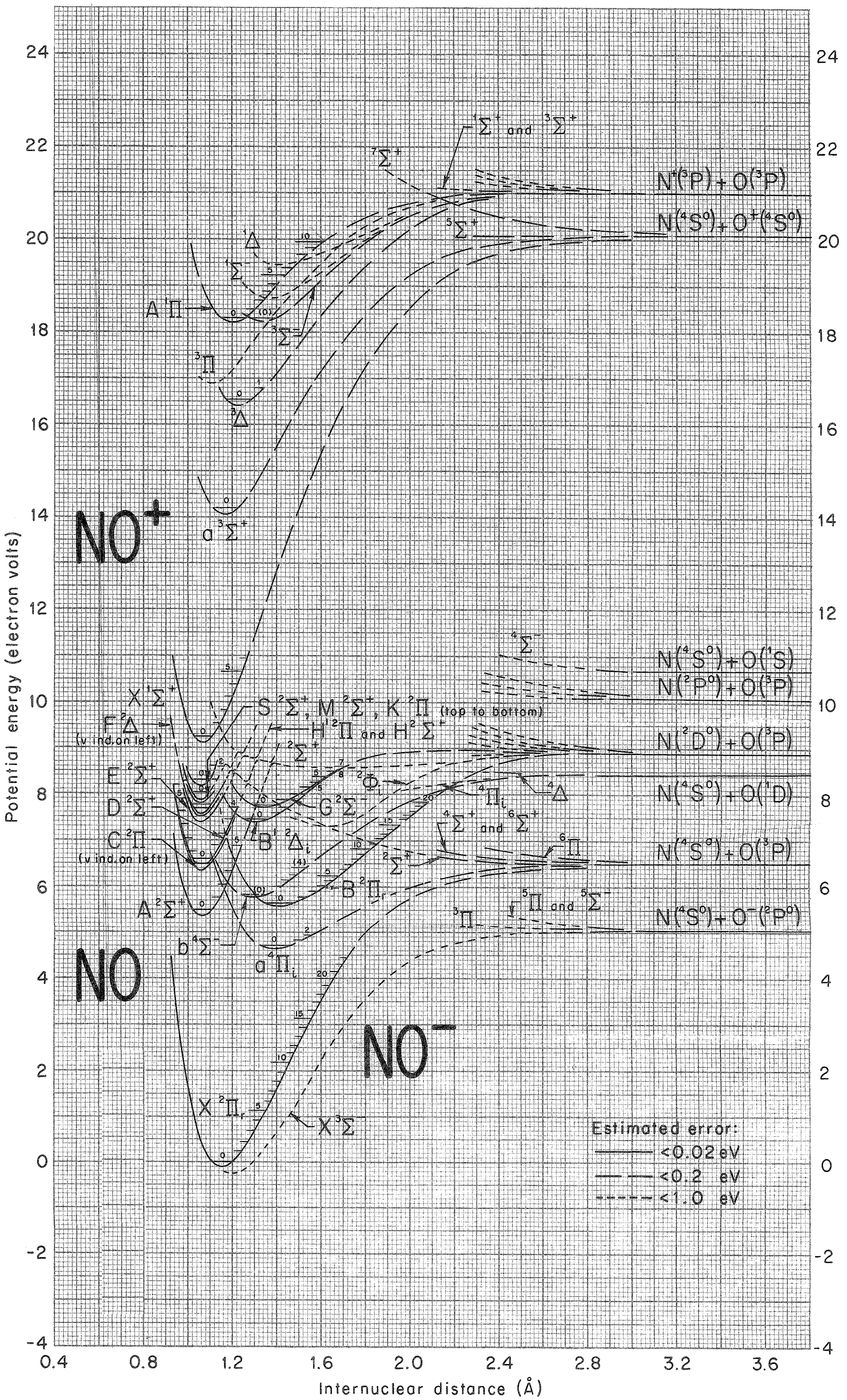

Fig. 2—Potential-energy curves for NO^-, NO and NO^+

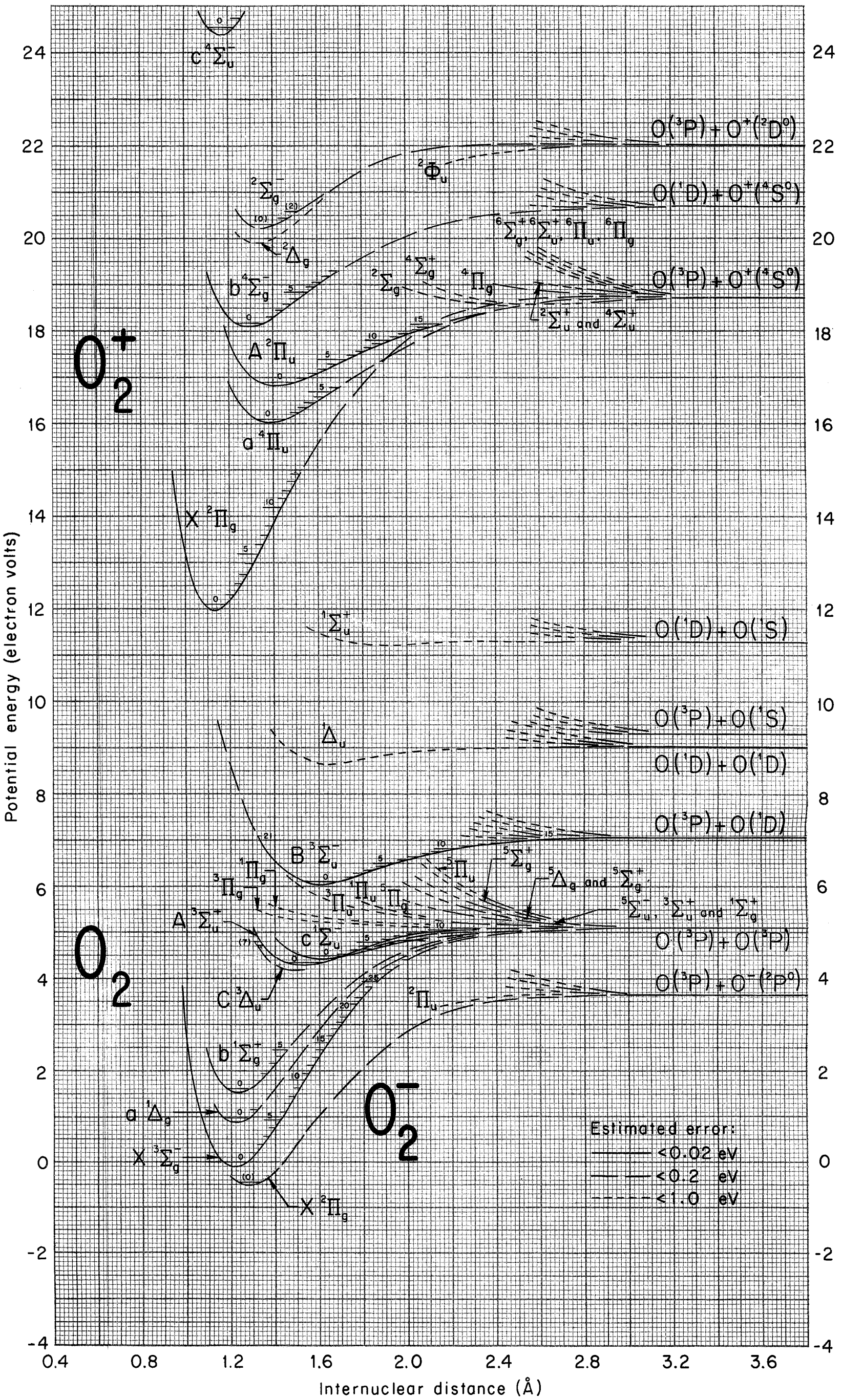

Fig. 3—Potential-energy curves for O_2^-, O_2 and O_2^+